ELSEVIER

PERGAMON MATERIALS SERIES 14

SELF-DIFFUSION AND IMPURITY DIFFUSION IN PURE METALS

HANDBOOK OF EXPERIMENTAL DATA

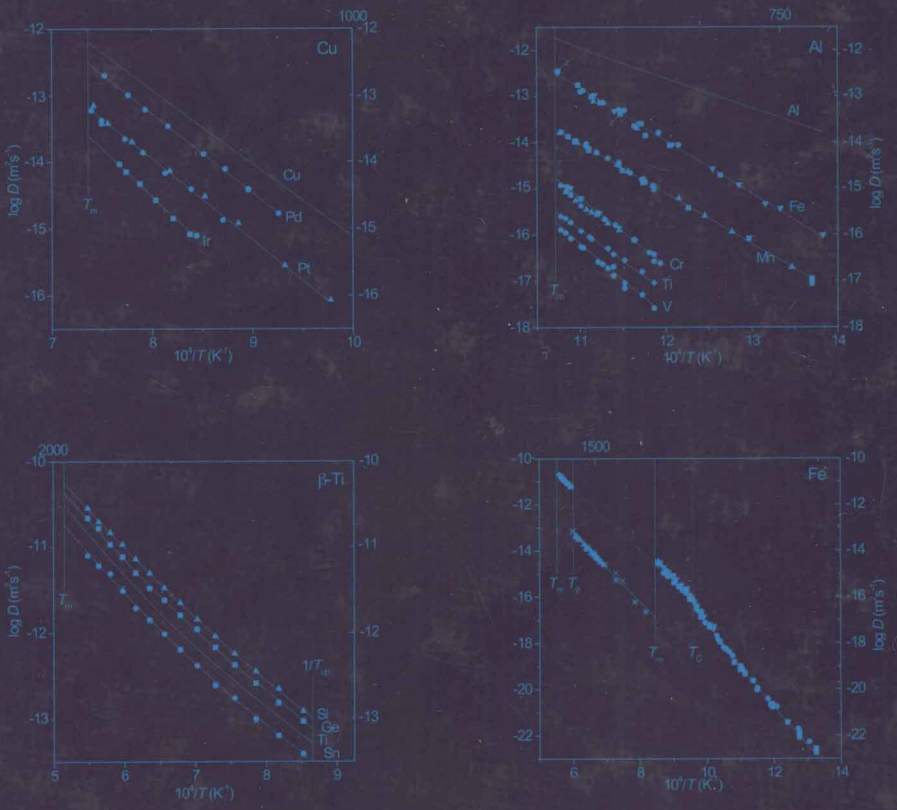

GERHARD NEUMANN AND
CORNELIS TUIJN

SELF-DIFFUSION AND IMPURITY DIFFUSION IN PURE METALS: HANDBOOK OF EXPERIMENTAL DATA

By

GERHARD NEUMANN
Institut für Physikalische Chemie
Freie Universität Berlin

CORNELIS TUIJN
Department of Physics
Universiteit van Amsterdam

ELSEVIER

Amsterdam • Boston • Heidelberg • London • New York • Oxford
Paris • San Diego • San Francisco • Singapore • Sydney • Tokyo
Pergamon is an imprint of Elsevier

Pergamon is an imprint of Elsevier
Linacre House, Jordan Hill, Oxford OX2 8DP, UK
Radarweg 29, PO Box 211, 1000 AE Amsterdam, The Netherlands
525 B Street, Suite 1900, San Diego, CA 92101-4495, USA

First edition 2009

British Library Cataloguing in Publication Data
A catalogue record for this book is available from the British Library

Library of Congress Cataloging-in-Publication Data
A catalog record for this book is available from the Library of Congress

ISBN: 978-1-85617-511-1

For information on all Pergamon publications
visit our website at books.elsevier.com

Printed and bound in Great Britain

09 10 11 12 13 10 9 8 7 6 5 4 3 2 1

SELF-DIFFUSION AND IMPURITY DIFFUSION IN PURE METALS: HANDBOOK OF EXPERIMENTAL DATA

PERGAMON MATERIALS SERIES

Vol. 1 **CALPHAD** by N. Saunders and A. P. Midownik
Vol. 2 **Non-Equilibrium Processing of Materials** edited by C. Suryanarayana
Vol. 3 **Wettability at High Temperatures** by N. Eustathopoulos, M. G. Nicholas and B. Drevet
Vol. 4 **Structural Biological Materials** edited by M. Elices
Vol. 5 **The Coming of Materials Science** by R. W. Cahn
Vol. 6 **Multinuclear Solid-State NMR of Inorganic Materials** by K. J. D. MacKenzie and M. E. Smith
Vol. 7 **Underneath the Bragg Peaks: Structural Analysis of Complex Materials** by T. Egami and S. J. L. Billinge
Vol. 8 **Thermally Activated Mechanisms in Crystal Plasticity** by D. Caillard and J. L. Martin
Vol. 9 **The Local Chemical Analysis of Materials** by J. W. Martin
Vol. 10 **Metastable Solids from Undercooled Melts** by D. M. Herlach, P. Galenko and D. Holland-Moritz
Vol. 11 **Thermo-Mechanical Processing of Metallic Materials** by B. Verlinden, J. Driver, I. Samajdar and R. D. Doherty
Vol. 12 **Phase Transformations Examples from Titanium and Zirconium Alloys** by S. Banerjee and P. Mukhopadhyay
Vol. 13 **Intermetallic Chemistry** by R. Ferro and A. Saccone

PREFACE

The most recent comprehensive data collection on diffusion in metals was published in 1990 (Landolt-Börnstein NS III 26). In the meantime numerous new results on self-diffusion and impurity diffusion in solid metals have been published. Especially, impurity diffusion coefficients measured by means of electron probe microanalysis (EPMA), Rutherford backscattering (RBS) and heavy ion backscattering (HIRBS) have been reported. Moreover, a number of earlier results had to be reassessed.

The present comprehensive data collection is based on a critical valuation of the hitherto published data and and aims at being the most complete data collection on this subject at this moment.

The authors wish to thank the employees of the libraries of the Hahn-Meitner Institute in Berlin and of the Library of Science of the University of Amsterdam, for the supply of many earlier articles, and in particular Mrs. Marijke Duyvendak, for searching in libraries all over the world.

The authors are also grateful to Professor Denis Ablitzer (Nancy), Professor Dieter Bergner (Freiberg), Professor Yoshiaki Iijima (Sendai) and Professor Jean Philibert (Orsay) for providing reprints and copies of a number of publications.

Gerhard Neumann
Cornelis Tuijn
January 2008

CONTENTS

CHAPTER 0

Introduction

The first diffusion investigation in metals was that of Au in lead by Roberts-Austen in 1896. Between 1930 and 1935 further impurity and self-diffusion investigations in lead had been performed by Hevesy, Seith and coworkers (for references see Chapter 4). Later on, when the first artificial radioisotopes became available, self-diffusion in gold [00.01, 00.02], copper [00.03, 00.04], silver [00.05] and zinc [00.06] was measured. Systematic investigations on self-diffusion and impurity diffusion in solid metals started with the availability of numerous artificial radioisotopes after the Second World War. Results of non-radioactive investigations represented a minority in that period. In the last two decades, however, the fraction of non-radioactive measurements has markedly increased.

The last comprehensive data collection in metals and alloys was published in 1990 [00.07], including self-diffusion [00.08] and impurity diffusion [00.09] in metals. Since then numerous further investigations have been performed, especially in aluminum, α- and β-titanium, α-zirconium and α-iron. Moreover, a large number of earlier investigations had to be reassessed.

The present collection contains data of self-diffusion and impurity diffusion in metals. Diffusion in silicon, germanium, selenium and tellurium is not topic of the present collection. Diffusion of C, N and O in metals is also not included in the present data collection. Data of these impurities are compiled in Ref. [00.10].

0.1. EXPERIMENTAL TECHNIQUES

Numerous methods have been developed for the measurement of self-diffusion and impurity diffusion coefficients in metals. The most reliable experimental data can be obtained with the aid of tracer sectioning techniques by means of radioactive isotopes. Also a number of non-radioactive investigation methods permits the determination of impurity diffusion coefficients. Furthermore, some non-destructive techniques, especially scattering experiments, were used for diffusion investigations. The methods for measuring diffusion coefficients have been described in detail in a number of reviews [01.01–01.04]. In the present chapter the most frequently applied measuring methods are briefly described.

Diffusion investigations are performed in a concentration gradient. The temporal and local change of the tracer concentration $c(x,y,z,t)$ is described by Fick's second law

$$\frac{dc}{dt} = D\Delta c \tag{01.01}$$

The serial sectioning technique consists of measuring the activity of thin sections removed from the sample parallel to the surface, i.e. normal to the diffusion direction. This simplifies Eq. (01.01) to the one-dimensional form

$$\frac{dc}{dt} = D\frac{d^2c}{dx^2} \tag{01.02}$$

The solutions of Eqs. (01.01) and (01.02) depend on the initial and boundary conditions, respectively, and are collected in Refs. [01.05, 01.06].

0.1.1 Radiotracer techniques

The experimental details of the measurement of tracer diffusion coefficients are extensively reviewed by Rothman [01.02]: sample preparation, tracer deposition, annealing, temperature measurement, determination of the effective annealing time, sectioning and counting (for further reviews see Refs. [01.07, 01.08]).

In the present chapter the different sectioning techniques and the respective range of measured diffusion coefficients are compared. Especially the penetration plots give informations concerning the accuracy of D. A number of possible sources in the determination of D has to be taken into consideration:

- Falsification of the penetration profile owing to surface diffusion contributions can be avoided by removing a layer of some $\sqrt{Dt}$ thickness from the side faces of the samples.
- Temperature measurements by use of thermocouples (mainly Pt/Pt(Rh), Ni(Cr)/Ni) may lead to errors of ± 1.5 K, which corresponds to an uncertainty of $\pm 3\%$ in D. Temperature measurements using optical pyrometry lead to distinctly larger uncertainties. An error of about 30 K in T at 3,000 K corresponds to an uncertainty of about 20% in D.
- For the determination of the accurate diffusion time a correction for the heating and cooling period has to be performed [01.09].

Macrosectioning techniques

Direct profile measurements. The most accurate methods for the measurement of diffusion coefficients are sectioning techniques using precision lathe and microtome, which permits the removal of sections of only a few microns thick. The section thickness is determined by weighing. Microtome and lathe sectioning is suited for ductile but not too soft materials.

If an infinitesimally thin layer ($\ll \sqrt{Dt}$) of radiotracers is deposited on the flat surface of the sample, the initial and boundary conditions for the semi-infinite

diffusion couple are

$$\lim_{\delta \to 0} c(x,0) = \frac{M}{2\delta} \text{ for } |x| \leq \delta, \text{ i.e. } \infty \text{ for } x = 0$$
$$\lim_{\delta \to 0} c(x,0) = 0 \text{ for } |x| > \delta, \text{ i.e. } 0 \text{ for } x \neq 0 \tag{01.03}$$

where M is the deposited amount in g/m^2 and δ the layer thickness. The so-called *thin film solution* of Eq. (01.02) yields [01.05]:

$$c(x,t) = \frac{M}{2\sqrt{\pi D t}} \exp\left(-\frac{x^2}{4Dt}\right) \tag{01.04}$$

which is linear in ln c against x^2 (see Figure 01.01). The slope of this plot yields D.

Deviations from linearity and the respective error sources are treated in a special section (see below). Diffusion coefficients with an uncertainty of only a few percent can be obtained with the aid of microtome and lathe sectioning.

Grinding or lapping is the standard method of sectioning brittle materials. Emery or abrasive SiC papers as well as diamond paste are used for 3–100 µm sections. The section thickness is determined by weighing the sample after each section that has been removed. Equation (01.04) describes the penetration plot.

Lathe, microtome and grinder sectioning permit the measurement of diffusion coefficients larger than $10^{-16}\,m^2\,s^{-1}$ or temperatures higher than about $0.7\,T_m$ (T_m is melting temperature), grinding with SiC papers diffusion coefficients as small as $10^{-17}\,m^2\,s^{-1}$.

Residual activity method. An alternative method for the determination of D using grinding was proposed by Gruzin [01.11]. Instead of measuring the activity of the sections the residual activity of the sample after removing the sections is measured. Then the activity of the n-th section is the difference of the residual activities after removing $n-1$ and n sections. The solution of Eq. (01.02) yields [01.05]

$$\frac{A_n}{2A_0} = \frac{1}{\sqrt{Dt}} \operatorname{erfc}\left(\frac{x}{2\sqrt{Dt}}\right) \tag{01.05}$$

where A_0 is the initial counting rate and A_n the remaining activity after the removal of n sections. erfc(z) is the complementary error function

$$\operatorname{erfc}(z) = 1 - \operatorname{erf}(z)$$

see Figure 01.02. D can also be derived from the Gaussian plot

$$\ln \frac{\partial A}{\partial x} = \text{const} - \frac{x^2}{4Dt} \tag{01.06}$$

The plot of the inverse function of erfc(z) $= A_n/2A_0$, i.e. $\operatorname{erfc}_{(-1)}(A_n/2A_0)$ against x is linear if the initial and boundary conditions are properly fulfilled (see Figure 01.02).

The Gruzin method is considered as less precise than the before-mentioned sectioning techniques. Only if the tracer is a hard γ radiator the absorption is

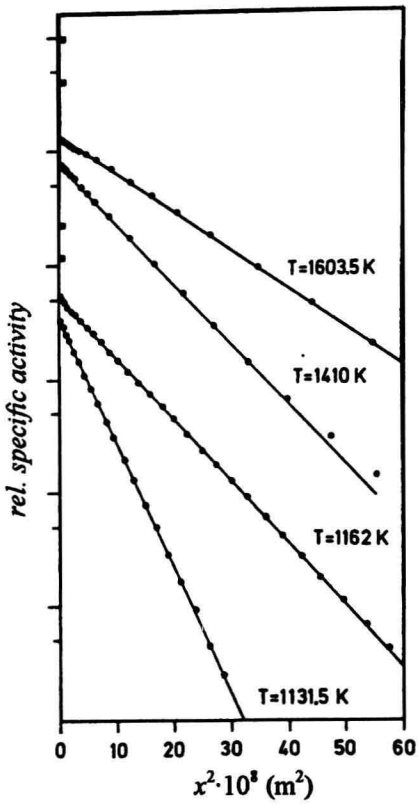

Fig. 01.01 Impurity diffusion of ^{95}Nb in α- and γ-iron. Microtome sectioning (2–5 μm sections) (from Ref. [01.10]).

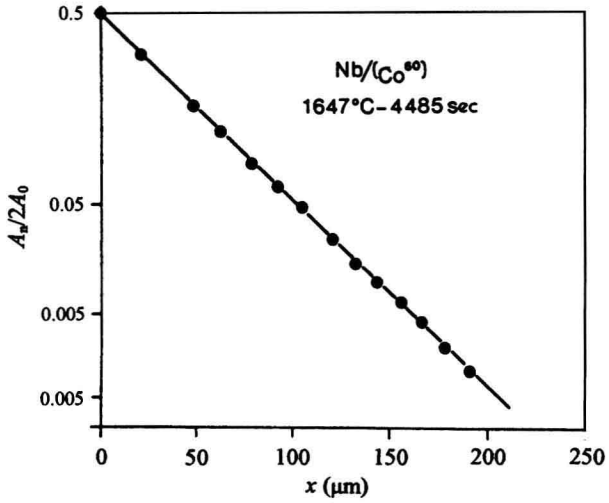

Fig. 01.02 Impurity diffusion of ^{60}Co in niobium. Residual-activity measurement. Profile fitted to Eq. (01.05) (from Ref. [01.12]).

negligible. Otherwise the linear absorption coefficient of the radiation has to be measured accurately. The method is mainly used in grinder sectioning investigations on polycrystalline materials.

Surface activity decrease method. The measurement of the decrease of the surface activity (or simple absorption method) before and after the diffusion anneal can also be used for the determination of D [01.13, 01.14]. This method is based on the surface activity decrease during the anneal which is caused by the absorption of the radiation of the tracer material diffused into the bulk. As in the Gruzin technique the absorption coefficient of the radiation has to be known. The method is regarded as less reliable than the sectioning techniques because it needs assumptions about the concentration profile. Particularly, errors can arise from tracer loss, oxide hold-up and short-circuiting contributions (grain boundary and dislocation contributions).

A variant of the simple absorption method is the Kryukov absorption method [01.15]. The radioactivity from both front face and back face of a very thin sample is counted after the diffusion anneal. So, D can be evaluated without the knowledge of the absorption coefficient.

Autoradiography. Autoradiography has also been used for the measurement of diffusion coefficients [01.16, 01.17]. The tracer penetration is derived from an autoradiograph taken from a flat cut at a small angle to the plane where the tracer was deposited. Although this cannot be considered a highly precise technique, for Sb diffusion in copper at least at high temperatures good agreement with the lathe sectioning data was observed [01.18].

Microsectioning techniques

Diffusion coefficients smaller than $10^{-17}\,m^2\,s^{-1}$ can be measured with the aid of chemical and electrochemical techniques. Sectioning by chemical dissolution permits the removal of 100 nm thick layers [01.19]. Sections between 10 and 100 nm can be obtained by mechanically stripping of electrochemically anodized layers [01.20]. This enables the measurement of diffusion coefficients as small as $10^{-22}\,m^2\,s^{-1}$ at temperatures of about 0.5 T_m [01.21]. Lundy and coworkers have used this method for the investigation of self-diffusion and impurity diffusion in β-Ti, β-Zr, Nb, Ta and W.

Diffusion coefficients as small as $10^{-23}\,m^2\,s^{-1}$ at $T \approx 0.4\,T_m$ can be obtained by application of sputtering methods. Sections smaller than 1 nm can be removed by ion bombardment (ion-beam sputtering, IBS). A concentration-depth profile can be measured by collecting the sputtered-off radiotracer material [01.22, 01.23] or by selecting and counting the sputtered-off material in a mass spectrometer (secondary-ion mass spectroscopy, SIMS) [01.24]. The depth of the profile (total crater depth) is measured by optical interference methods after sectioning has been completed. The thickness of the sections is determined under the assumption that the material is removed uniformly as a function of time. To avoid short-circuiting contributions single crystals with small dislocation densities have to be

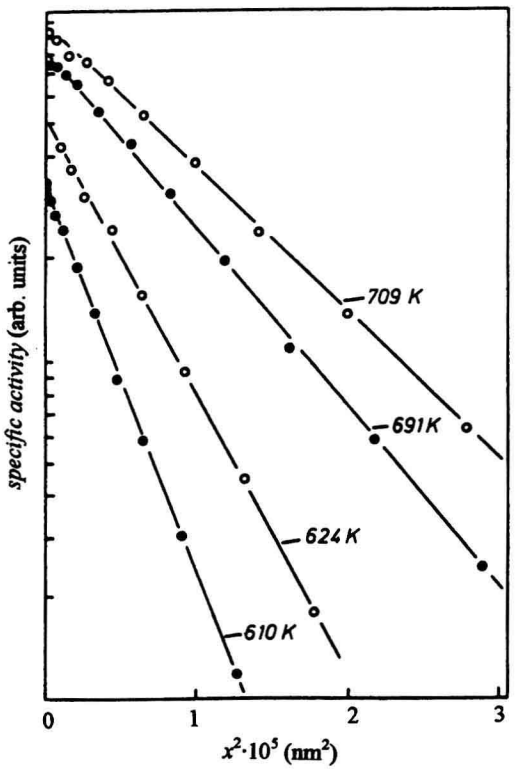

Fig. 01.03 Impurity diffusion of ^{114m}In in silver. Ion-beam sputtering (from Ref. [01.25]).

used. The depth resolution of the sputter sectioning technique is limited which results from roughening and atomic mixing [01.24]. Roughening reduces the depth resolution because atoms are sputtered simultaneously from different depths with different concentrations of tracers. Mixing of atoms from different depths is a consequence of the lattice damage caused by the sputter ions. Roughening increases with depth. The accuracy of diffusion coefficients measured by means of sputtering techniques is within 10–20%.

In Figures 01.03 and 01.04 the penetration profiles for In diffusion in silver [01.25] and Ni diffusion in copper [01.24] are shown. For ^{114m}In in silver Ar^+ ions with an energy of about 0.5 keV were used for sputtering. The penetration profiles are ranging from about 100–500 nm (see Figure 01.03). For Ni in copper single crystalline samples with inserted thin Ni layers are used. The sputter deposited Ni (monoatomic layer with initial distribution with a half-width of 11 nm) is covered by an epitaxial, almost monocrystalline layer of copper of about 100 nm. O_2^+ ions of 4 keV were used for sputtering. The penetration plots are smaller than 100 nm (see Figure 01.04).

IBS plus radiotracer counting permits the measurement of self-diffusion as well as impurity diffusion coefficients in the temperature range between about 0.4 and 0.6 T_m. Especially for self-diffusion in fcc metals the low-temperature

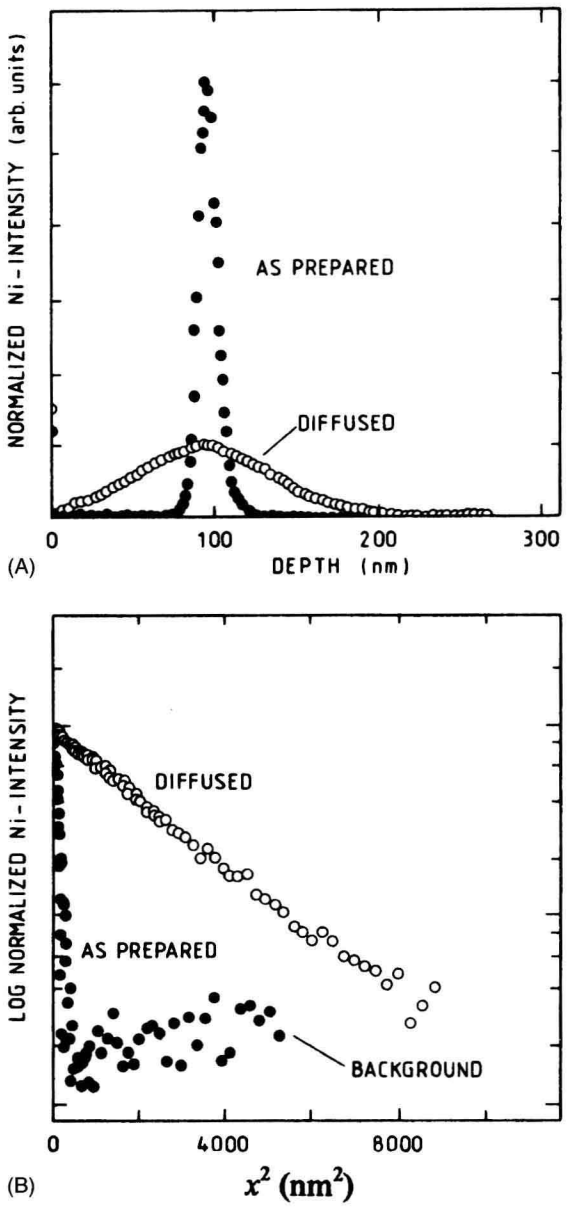

Fig. 01.04 Impurity diffusion of Ni in copper. Ion-beam sputtering and SIMS analysis (initial distribution with a half-width of 11 nm) (from Ref. [01.24]).

data detect the slight curvature of the Arrhenius plot of D and enables the evaluation of $D(T)$ in form of two-exponential fits (see Chapter 0.2). IBS plus SIMS analysis permits the measurement of impurity diffusion coefficients of elements which have no suitable radioisotopes.

Non-Gaussian diffusion profiles

Deviations from linearity of the ln c vs. x^2 plot, i.e. non-Gaussian profiles, are observed if the boundary conditions are not properly fulfilled or if other mechanisms like short-circuiting diffusion overlap the lattice diffusion. Non-Gaussian profiles are obtained, if

1) Grain boundaries or dislocations contribute to D (this contribution increases with decreasing temperature and decreasing grain diameter).
2) Oxide layers at the surface hinder the penetration of the tracer atoms.
3) Reduced solubility of impurities changes the boundary conditions.
4) Tracer atoms evaporate from the surface, which also changes the boundary conditions.

Short-circuiting contributions lead to an upward deviation from the Gaussian plot at deeper penetrations (see Figure 01.05). Grain-boundary diffusion results in a proportionality between ln c and $x^{6/5}$ [01.27, 01.28]. The short-circuiting contribution can be eliminated mathematically if the penetration plot is fitted to [01.29]

$$c(x,t) = \frac{M}{2\sqrt{\pi Dt}} \exp\left(-\frac{x^2}{4Dt}\right) + A\exp(-Bx^{6/5}) \qquad (01.07)$$

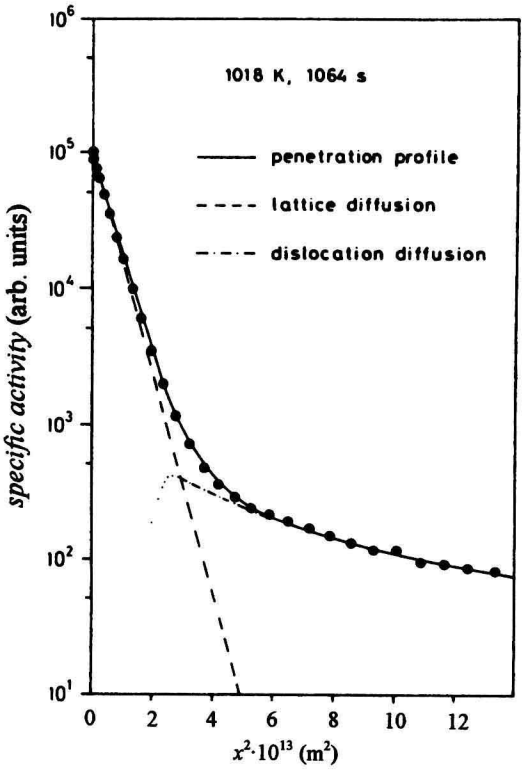

Fig. 01.05 Self-diffusion of ^{59}Fe in α-iron. Penetration profile with dislocation tail (from Ref. [01.26]).